Edinburgh Research Explorer

Anonaine from Annona crassiflora inhibits glutathione S-transferase and improves cypermethrin activity on Rhipicephalus (Boophilus) microplus (Canestrini, 1887)

1   Anonaine from *Annona crassiflora* inhibits glutathione S-transferase and improves

2   cypermethrin activity on *Rhipicephalus (Boophilus) microplus* (Canestrini, 1887)

3

4   Wallyson André dos Santos Bezerra[a], Caio Pavão Tavares[b], Cláudia Quintino da

5   Rocha[c], Itabajara da Silva Vaz Junior[d], Paul A. M. Michels[e], Livio Martins Costa

6   Junior[b], Alexandra Martins dos Santos Soares[a*]

7

8   [a]Laboratório de Bioquímica Vegetal, Departamento de Engenharia Química, Universidade

9   Federal do Maranhão, São Luís, MA, Brasil.

10   [b]Laboratório de Controle de Parasitos, Departamento de Patologia, Universidade Federal do

11   Maranhão, São Luís, MA, Brasil.

12   [c]Laboratório de Química de Produtos Naturais, Departamento de Química, Universidade Federal

13   do Maranhão, São Luís, MA, Brasil.

14   [d]Faculdade de Veterinária e Centro de Biotecnologia, Universidade Federal do Rio Grande do

15   Sul, Porto Alegre, RS, Brazil.

16   [e]Centre for Immunity, Infection and Evolution and Centre for Translational and Chemical

17   Biology, School of Biological Sciences, The University of Edinburgh, Edinburgh, United

18   Kingdom.

19   [*]Corresponding author: alexandra.soares@ufma.br

20

21

22   **Graphical Abstract**

Anonaine

Cypermethrin

Annona crassiflora

In silico R. microplus **GST inhibition by anonaine**

In vitro R. microplus **GST inhibition by anonaine**

Larvicidal effect

23
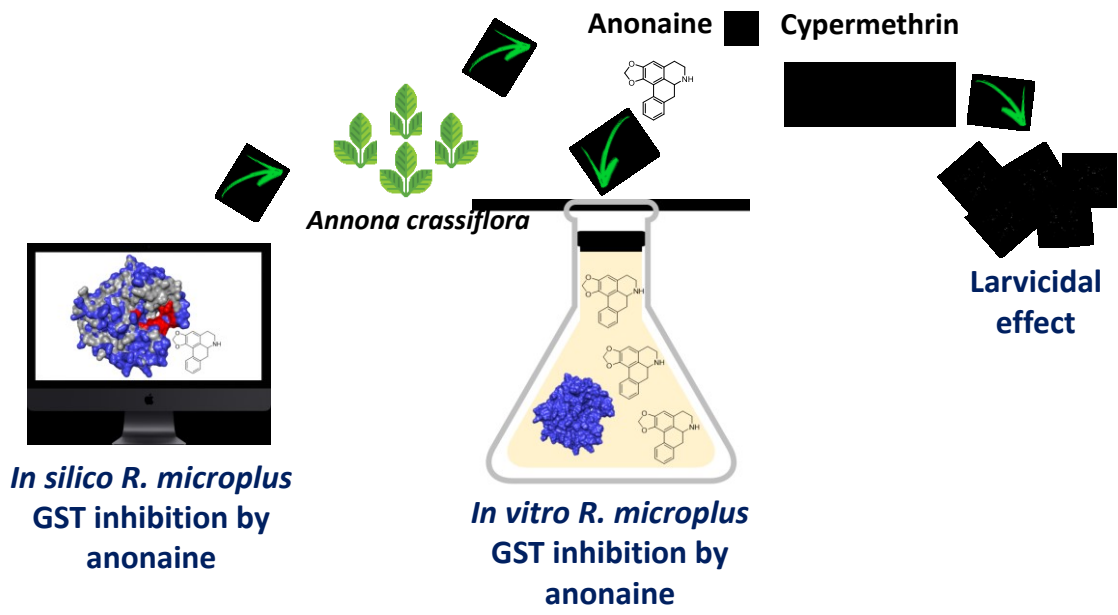
Abstract

Rhipicephalus (Boophilus) microplus (Canestrini, 1887) is one of the most important ectoparasites of cattle, causing severe economic losses in tropical and subtropical regions of the world. The selection of resistance to the most commonly used commercial acaricides has stimulated the search for new products for tick control. The identification and development of drugs that inhibit key tick enzymes, such as glutathione S-transferase (GST), is a rational approach that has already been applied to other parasites than ticks. In this context, alkaloids such as anonaine display several biological activities, including an acaricidal effect. This study aimed to assess the specific inhibition of the *R. microplus* GST by anonaine, and analyze the effect on ticks when anonaine is combined with cypermethrin. For this purpose, a molecular docking analysis was performed using an *R. microplus* GST three-dimensional structure model with anonaine and compared with a human GST-anonaine complex. The absorption, distribution, metabolism, excretion, and toxicity properties of anonaine were also predicted. Then, for *in vitro* analyses, anonaine was isolated from *Annona crassiflora* (Martius, 1841) leaves. The inhibition of purified recombinant *R. microplus* GST (rRmGST) by anonaine and the effect of this alkaloid on cypermethrin efficacy towards *R. microplus* were assessed. Anonaine has a higher affinity to the tick enzyme than to the human enzyme *in silico* and has moderate toxicity, being able to inhibit, *in vitro*, rRmGST up to 37.5% in a dose-dependent manner. Although anonaine alone has no activity against *R. microplus*, it increased the cypermethrin effect on larvae, reducing the LC_{50} from 44 to 22 μg/mL. In conclusion, anonaine is a natural compound that can increase the effect of cypermethrin against *R. microplus*.

Keywords: Tick, plant alkaloid, GST inhibition, pyrethroid

1. Introduction

49   The cattle tick *Rhipicephalus (Boophilus) microplus* (Canestrini, 1887) poses a

50   severe economic threat to livestock producers through physical effects on infested

51   animals and diseases caused by the transmission of parasitic protists (Kumar et al., 2013).

52   It is estimated that *R. microplus* causes annual losses in the Brazilian cattle herd of up to

53   US$ 3.2 billion (Grisi et al., 2014).

54   Tick control is usually carried out through the repeated use of chemical acaricides,

55   such as synthetic pyrethroids (Kumar et al., 2013), which has led to increased selection

56   of acaricide resistance among tick populations, in addition to promoting contamination

57   of the environment and food products (Kaewmongkol et al., 2015).

58   Plants defend themselves against pests by producing several phytochemicals that

59   have been considered potential alternatives for tick control (Guneidy et al., 2014). For

60   instance, anonaine, an alkaloid present in the plant *Annona crassiflora* (Martius, 1841)

61   (Annonaceae), a tree native to the Brazilian Cerrado popularly known as "araticum", is a

62   bioactive compound displaying several biological properties, including antiparasitic

63   activity (Li et al., 2013).

64   Various inhibitors of enzymes have been studied to develop control methods against

65   parasites (Olivares-Illana et al., 2006; Braz et al., 2019; Cuevas-Hernándes et al., 2020),

66   based on the identification of molecules that induce selective inhibition of parasite over

67   host enzymes (Ahmad et al., 2008; Moraes et al., 2011; Ozelame et al., 2022). Based on

68   these previous results, the enzyme glutathione S-transferase (GST) can be considered a

69   target for developing antiparasitic drugs. Each of the GST subunits has its active site that

70   is composed of a glutathione (GSH) binding site (G site) and an electrophilic substrate

71   binding site (H site) (Prade et al., 1997). GSTs play an essential role in detoxifying

72   xenobiotics (Mannervik, 1985; Mannervik et al., 1988; Hamza and Dailey, 2012).

73   Compounds capable of inhibiting the tick's GST activity to interrupt its detoxification

74 system, could provide an alternative form of control (Guneidy et al., 2014; Ozelame et

75 al., 2022). As alkaloids are among the natural products capable of inhibiting GST

76 (Mangoyi et al., 2010; Azeez et al., 2012; Divya et al., 2014; Behera and Bhatnagar,

77 2019), anonaine is a potential candidate for the control of *R. microplus* through the

78 inhibition of this enzyme.

79 Recently, *in silico* techniques have facilitated the discovery of new drug candidates

80 (Alvarez, 2004; Choubey and Jeyaraman, 2016; Ganesan, 2016; Roche and Bertrand,

81 2016; Saramago et al., 2018). For instance, through molecular docking, drug candidates

82 can be recognized, and the potential for their optimization can be explored as molecular

83 interactions between ligands and target molecules can be analyzed and modelled

84 (Wadood et al., 2013).

85 Given the scientific and economic importance of the development of new acaricide

86 products against ticks and considering that GST is a target enzyme is a target enzyme

87 essential in the physiology of the ticks, this study used *in silico* and *in vitro* assessments

88 to analyze the potential use of anonaine as a specific tick GST inhibitor. By decreasing

89 the activity of this enzyme one can interfere with the detoxification of cypermethrin,

90 thereby increasing the effectiveness of this synthetic pyrethroid.

91

92 **2. Methodology**

93 **2.1 Construction and validation of the glutathione S-transferase (GST) model**

94 The GST sequence of *R. microplus* (GenBank number AAL99403.1) was used as a

95 query sequence on the Phyre 2 server (Kelley et al., 2015), with normal modelling mode.

96 The created model was then validated using the PROCHECK 3.0 server (Laskowski et

97 al., 1993).

98

2.2 Anonaine structure and ADMET features.

The anonaine structure was obtained from the PubChem database (CID: 160597) in mol2 format and optimized in the Avogrado program (Hanwell et al., 2012). ADMET (Absorption, Distribution, Metabolism, Excretion, and Toxicity) properties of anonaine were analyzed using PreADMET software (Kwang, 2005). The ADMET analyses were carried out according to the specific classifications and parameters (Van De Waterbeemd and Gifford, 2003; Tong et al., 2021).

2.3 Molecular docking of GST from *R. microplus* and human with anonaine

To analyze the potential inhibitory activity of anonaine to the *R. microplus* enzyme, molecular docking was carried out in the H-site of both a human and a tick GST, using Molegro Virtual Docker 6.0 (MVD) software. The structure of the human GST complexed with the inhibitor N11 (6-[(7-nitro-2,1,3-benzoxadiazol-4-yl)sulfanyl]hexan-1-ol) was obtained from the Protein Data Bank (www.rcsb.org) at 1.8 Å resolution (PDB ID: 3IE3 – chain A).

The human GST structure was employed for re-docking simulations by fitting the N11 to the enzyme using 32 docking protocols. For this purpose, statistical analysis of coupling results and scoring functions (SAnDReS) were used (Xavier et al., 2016). The algorithms were valid if the re-docking results had a root square mean deviation (RSMD) less than 2 Å from the original structure (Yusuf et al., 2008). The re-docking protocol result with the lowest RSMD was selected for molecular docking simulations.

The structures of anonaine and human GST were imported into the MVD workspace in 'mol2' format. The GST's structures were prepared (always assigning bonds, bond orders and hybridization, charges and tripos atom types; always creating explicit hydrogens and always detecting flexible torsions in ligands) using the utilities provided

124 in MVD. Molecular docking was carried out inside a virtual docking sphere of 15 Å radius

125 and the following centre coordinates: X: 6.06; Y: 3.61; Z: 28.00Å. Ten independent runs

126 were conducted, and the results were expressed in MolDock score. The more negative the

127 number, the better the binding (Hall Jr and Ji, 2020). The same parameters were used to

128 perform the molecular docking of anonaine onto the *R. microplus* GST. It is noteworthy

129 that after superimposing the structures of the human and tick GSTs used in this study, an

130 RMSD of 1.1 Å was obtained while their sequences have an amino-acid identity of 28.8%.

131 The best pose of both GSTs with anonaine was visualized and analyzed using the

132 PyMOL Molecular Graphics System v1.3 program (http://www.pymol.org/) and the

133 residues of the GSTs interacting with anonaine were analyzed using Discovery Studio

134 Visualizer software.

135 The *R. microplus* and human (Linnaeus, 1758) GST sequences were aligned using

136 Clustal Omega software (Sievers et al., 2011), and the residues interacting with anonaine

137 (taken from the docking results with both GSTs) were highlighted in the alignment.

138

139 **2.4 Extraction and purification of anonaine**

140 The extraction and purification procedure followed a methodology adapted from

141 Chen et al. (2001). Leaves of *Annona crassiflora* were collected at Parque Nacional

142 Chapada das Mesas (07°07'47.1" S, 4°25'36.8" W), Carolina, Maranhão, Brazil, April

143 2018. A specimen (Exsiccate number MG 222438) was deposited in the Museu Paraense

144 Emílio Goeldi (MPEG) or Goeldi Museum, located in Belém, Pará, Brazil.

145 The leaves were dried in a circulating air oven at 50 ºC, ground (300 g), and subjected

146 to cold extraction using initially petroleum ether and then methanol (3 x 1 L, each),

147 resulting in 15.54 g of Ethereal Extract and 35.45 g of Methanolic Extract, respectively.

148 The analysis by thin-layer chromatography (TLC), using Dragendorff reagent, indicated

149 the presence of alkaloids in the methanolic extract. Therefore, about 10 g of the

150 methanolic extract was subjected to conventional acid-base treatment, yielding the

151 alkaloid enriched fraction (m: 0.57 g).

152 A part of the fraction (0.4 g) was subjected to chromatographic fractionation in a

153 silica gel column chromatography previously treated with a 5% NaHCO$_3$ solution and

154 eluted with gradients of petroleum ether: CH$_2$Cl$_2$, then gradients of CH$_2$Cl$_2$: EtOAc, and

155 finally gradients of EtOAc: CH$_3$OH, resulting in 50 fractions of 25 mL each. The obtained

156 fractions were analyzed by TLC in different solvent systems and gathered into 7 groups.

157 Group 3 (40.5 mg) was subjected to TLC using CH$_2$Cl$_2$: MeOH (8.0:2.0, v/v) as eluent,

158 and a single spot was found on the plate. The identification of anonaine was done by

159 comparison with standards and analysis of the mass spectrum.

160

161 **2.5 Expression and purification of glutathione S-transferase of *Rhipicephalus***

162 ***microplus* (r*Rm*GST)**

163 A DNA fragment containing the entire coding sequence of a *R. microplus* GST was

164 cloned in previous studies (Vaz et al., 2004; Ndawula et al., 2019). Then, the recombinant

165 GST (r*Rm*GST) was expressed and purified as previously described (Ndawula et al.,

166 2019). Briefly, *Escherichia coli* (Migula 1895) BL21(DE3) was transformed with

167 plasmid and the r*Rm*GST expression (in SOB medium) was induced by 1 mM IPTG

168 (isopropyl-beta-D-thiogalactopyranoside, Thermo Fisher Scientific, Waltham, MA,

169 USA) for 6 or 18 h at 37 °C. The culture was centrifuged at 16,000 x g for 10 min at 4 °C

170 and the pellet was washed with PBS 7.2 and lysed using an ultrasonic homogenizer with

171 5 cycles of 30 pulses for 30 s (Pulse Sonics Vibra-cell VCX 500- 700, Sonics & Materials,

172 Inc., Newtown, CT, USA).

173   The supernatant was loaded onto an affinity chromatography column of GSTrap 4B

174   (GE Healthcare, Chicago, IL, USA), previously equilibrated with binding buffer (PBS

175   pH 7.4). After being washed with the same buffer, the rRmGST was eluted with 50 mM

176   Tris-HCl pH 8.0 containing 10 mM reduced glutathione (GSH). The expression and

177   purification of rRmGST were monitored by SDS–PAGE and western blotting using anti-

178   rRmGST rabbit serum (Ndawula et al., 2019).

179

180   **2.6   GST enzymatic activity and inhibition by anonaine**

181   The enzymatic activity of purified recombinant GST was determined using the

182   substrate 1-chloro-2,4-dinitrobenzene (CDNB) (Sigma-Aldrich, Saint Louis, MO, USA)

183   and 3,4-dichloronitrobenzene (DCNB) (Sigma-Aldrich) at 25 ºC with a VersaMax™

184   Microplate Reader. Readings were performed at 340 nm for 30 min at 15 s intervals, as

185   previously described (Vaz et al., 2004; Habig et al., 1974). Substrates CDNB 3 mM and

186   DCNB 1 mM were diluted in methanol and added to the reaction mixture containing 100

187   mM potassium phosphate buffer, pH 6.5, 1 mM EDTA, and 3 mM GSH. Tests were

188   performed in 96-well microplates with 10 µL (0.7 µg) of recombinant protein in a total

189   volume of 100 µL. The background activity, which was subtracted from the data, was

190   determined using buffer, GSH, and CDNB, without enzyme.

191   For the inhibition tests, anonaine was diluted in 1% DMSO at 10 mg/mL (stock

192   solution). The inhibition of GST by anonaine was carried out at concentrations in the

193   range of 0.075 to 0.5 mg/mL. Inhibition tests were with 10 µL of recombinant protein in

194   100 µL of total volume. The assay in which anonaine was replaced by PBS represented

195   100% enzymatic activity. As a negative control, GST, CDNB, GSH, and DMSO (0.1%)

196   were used. The assays were performed in two independent assays, each in duplicate.

197

2.7 Ticks

Ticks of the Santa Rita strain were collected from naturally infested Girolando cattle on a farm located in the municipality of Santa Rita (03º08'37"S, 44º19'33"W), MA, Brazil, and maintained through artificial infestation on calves at the facilities of the Federal University of Maranhão (UFMA). This study was approved by the Ethics Committee on Animal Experimentation of UFMA, Brazil, under protocol number 23115.004153/2022-58.

2.8 Larval immersion test

The larval immersion test was performed according to Klafke et al. (2006), in triplicate. From the anonaine stock solution (10 mg/mL), solutions at 0.5 and 0.1 mg/mL final concentrations, in 1% ethanol and 0.02% Triton X-100 were tested. Cypermethrin was prepared at 20 mg/mL (stock solution) in 1% ethanol and 0.02% Triton X-100 and tested at 3.0, 1.2, 0.48, 0.19, 0.07, 0.03, 0.0123, 0.004, 0.002 and 0.0008 mg/mL. Cypermethrin was combined with anonaine (same concentrations as described above) in the tests on tick larvae. The control group was treated with a 1% ethanol and 0.02% Triton X-100 solution.

Approximately 500 larvae were immersed for 10 min in a mixture of anonaine and cypermethrin and transferred to a filter paper base. Then, approximately 100 larvae were transferred to a clean filter paper package (8.5 × 7.5 cm) closed with plastic clips. The packets were incubated for 24 h at 27 ± 1 °C with relative humidity $\geq 80\%$. Ticks were observed for 5 min. Dead (no movement) and alive larvae were manually counted. The tests were carried out in triplicate.

2.9 Adult immersion test (AIT)

223   For the adult immersion test (AIT) (Drummond et al., 1973), anonaine (at 0.5 and 0.1

224   mg/mL final concentrations) and cypermethrin (3.7 mg/mL final concentration) were

225   prepared as previously described and mixed in a solution. The tests were carried out in

226   triplicate.

227   Engorged females of *R. microplus* with homogeneous body mass (n = 180) were

228   divided into six groups (n = 10) as follows: 1) Control: 1% ethanol and 0.02% Triton X-

229   100 solution (v/v); 2) 3.7 mg/mL cypermethrin; 3) 3.7 mg/mL cypermethrin and 0.1

230   mg/mL anonaine; 4) 3.7 mg/mL cypermethrin and 0.5 mg/mL anonaine; 5) 0.1 mg/mL

231   anonaine; 6) 0.5 mg/mL anonaine. The cypermethrin concentration used in AIT was

232   determined by Ghosh et al. (2017). Ticks of each group were immersed in their respective

233   solution for five minutes, washed, and dried on absorbent paper.

234   The engorged females from each group were incubated at 27 ± 1 ºC and RH $\geq 80\%$,

235   for 15 days. After weighing the collected eggs and incubating them for 25 days at the same

236   temperature and humidity, the percentages of reduction in both oviposition and hatching

237   were assessed (Bennett, 1974; Lopes et al., 2013; Drummond et al., 1973).

238

239   **2.10 Statistical analysis**

240   For the enzymatic inhibition, larval, and adult immersion tests, all means obtained

241   were statistically analyzed by Analysis of Variance (ANOVA), followed by Tukey's test

242   ($p < 0.05$). The results were initially transformed to log (X), and the percentage of mortality

243   was normalized; subsequently, non-linear regression was performed to obtain the LC_{50}

244   (50% lethal concentration) values using GraphPad Prism 8.0.2 software (GraphPad Inc.,

245   San Diego, CA, USA). The significance of each concentration in the tests was determined

246   when the calculated confidence intervals do not overlap (Roditakis et al., 2005).

247

248   **3.   Results**

249   **3.1 Modelling of the three-dimensional (3D) structure of the GST of _R. microplus_**

250   The best template identified to prepare a reliable 3D structure model of _R. microplus_

251   GST (Supplementary Figure 1) using the Phyre2 web server was a _Gallus gallus_ GST

252   (Chain A, PDB:1C72), with 37.21% identity and 98% of coverage. The model dimensions

253   were X: 51,117, Y: 42,329, Z: 55,806 Å, with 100% modelling confidence. The

254   stereochemistry of the refined protein model revealed that of the 220 amino acid residues

255   of the GST of _R. microplus_, 91% were situated in the most favorable region of the

256   Ramachandran plot (Supplementary Figure 2).

257

258   **3.2 Re-Docking and Molecular Docking**

259   Re-docking protocol number 23 (Xavier et al., 2016), which uses plants score as

260   score function, and the iterated simplex (Ant Colony Optimization) as search algorithm,

261   resulted in an RMSD of 1.9 Å (docking RMSD value for human GST, PDB: 3IE3, with

262   N11 inhibitor) and was selected for molecular docking simulations in this study.

263   As a result of the molecular docking simulations, anonaine showed higher affinity to

264   the _R. microplus_ GST, with lower binding energy (-91.355) for this enzyme, compared to

265   the binding energy for the human GST (-85.249). The predicted interactions with the

266   amino acids from each of the GSTs (from the best pose for each GST) with anonaine are

267   highlighted in the alignment of the two GST sequences (Figure 1). Anonaine was found

268   to interact with the amino acids: Thr 10, Thr 11, Ala 12, Tyr 35, Glu 36, Phe 37, Gly 38,

269   Pro 39, Ala 40, Tyr 43, Pro 209, Met 211, Ala 212, Pro 213 of _R. microplus_ GST (Figure

270   1 and Supplementary Table 1).

271

272

Figure 1. Protein sequence alignment of the human GST (Hs.GST), (PDB ID: 3IE3-Chain A) and *Rhipicephalus microplus* GST (Rm.GST). Residues of human GST and tick GST interacting with anonaine are highlighted in yellow and blue, respectively.

3.3 ADMET analysis

The predicted ADMET properties of anonaine are shown in Supplementary Table 2. Anonaine is predicted to have good human intestinal absorption (96.493%), medium permeability in the Caco-2 cell model (47.681 nm/seg), low permeability in the Blood-Brain Barrier (BBB) model (0.9849), high permeability in the MDCK cellular system (> 25 nm/s), and a high plasma protein binding rate (65.565%). Regarding metabolism, anonaine is predicted to have inhibition ability on CYP2D6 and CYP3A4; to show mutagenic Ames toxicity and a low value of toxicity in the algae test (0.055948 mg/L), suggesting it will have moderate side effects to the mammals.

## 3.4 Isolation of alkaloid Anonaine and r*Rm*GST

289   Anonaine was isolated from the leaf methanolic extract of *A. crassiflora* as shown in

290   the HPLC analysis (Figure 2). The positive-mode mass spectrum showed a molecular ion

291   of m/z 266 $[M+H]^+$, with fragments of m/z 249, m/z 219, and m/z 191, indicating the

292   initial loss of the amine group and the CH_2O and CO groups.

293   A single protein band was observed in SDS-PAGE and western blot analyses of

294   r*Rm*GST purified by GSH affinity-column chromatography, confirming the enzyme's

295   identity and purity (above 97%) (Figure 3).
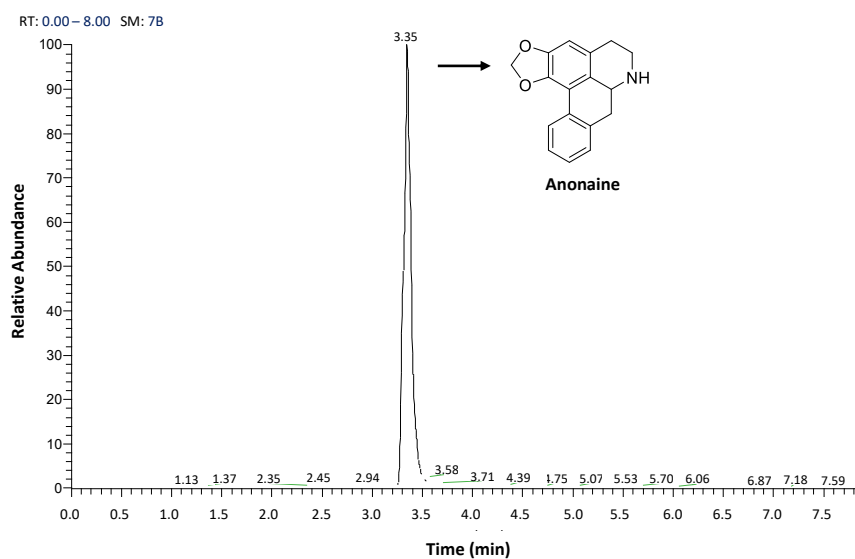
296

297 **Figure 2.** Chromatogram of total ions of anonaine, isolated from *Annona crassiflora*. Inset:

298 anonaine structure
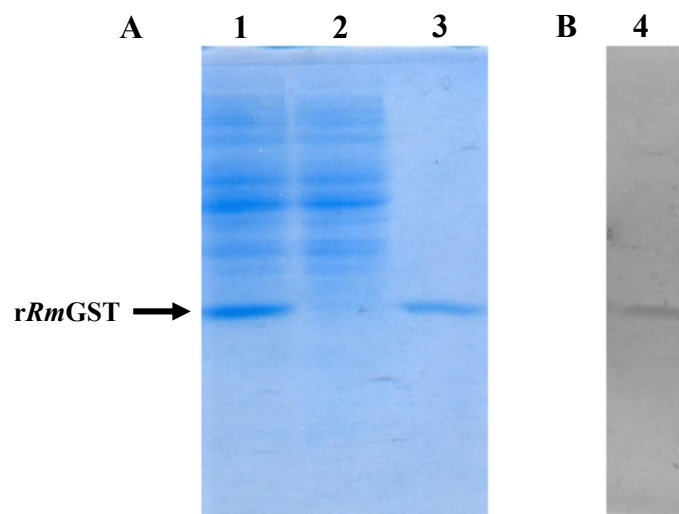
299

300 **Figure 3.** A) SDS-PAGE (12% gel, with electrophoresis performed under reducing conditions)

301 and B) Western blot of recombinant *R. microplus* GST. 1) Extract of *E. coli* cells expressing

302 r*Rm*GST; 2) Unbound fraction eluted in GSH chromatography; 3) Purified GST (r*Rm*GST); 4)

303 Western blot with anti-GST serum.

304

305 **3.5 *In vitro* inhibition of r*Rm*GST by anonaine**

306 The inhibitory activity of anonaine on the r*Rm*GST was determined at fixed

307 concentrations of CDNB (3 mM) and GSH (3 mM). It was observed that *R. microplus*

308 GST was inhibited by anonaine in a concentration-dependent manner (Figure 4).

309

310
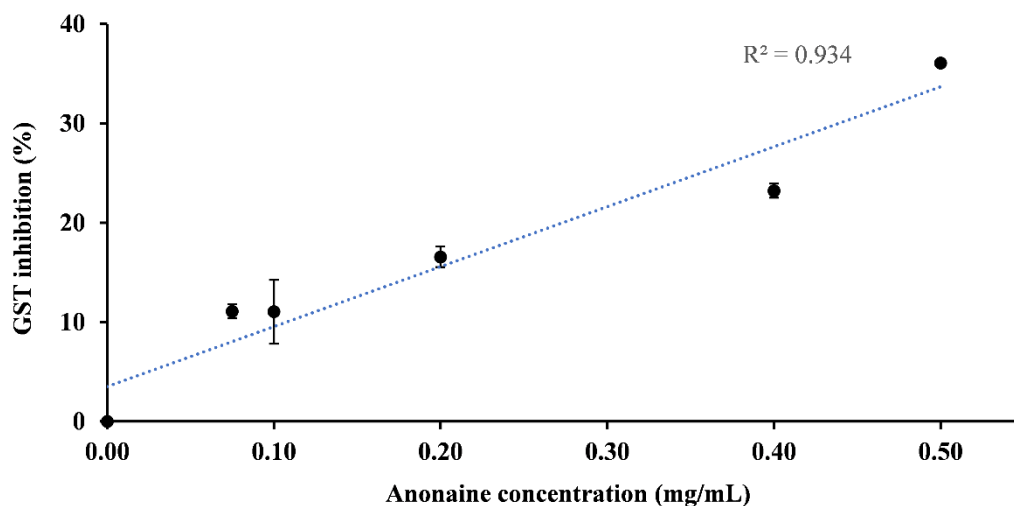
311 **Figura 4.** Inhibition curve for the anonaine on r*Rm*GST. Y-axis: percentage of GST inhibition;

312 X-axis: anonaine concentration in mg/mL.

313

314 **3.6 Effect of anonaine and cypermethrin on larvae and adults of *Rhipicephalus***

315 ***microplus***

316 Addition of anonaine increased the effect of cypermethrin on larvae; at a

317 concentration of 0.5 mg/mL resulting in a reduction in the cypermethrin's LC_{50} from 44

318 to 22 μg/mL, although anonaine itself did not show activity toward *R. microplus* larvae

319   at the tested concentrations (Table 1). Anonaine had an effect of 6.24±8.74% and

320   14.26±25.82% in engorged females at 0.1 and 0.5 mg/mL, respectively and did not alter

321   the cypermethrin effect on adults of *R. microplus*.

322

323   **Table 1.** Effect of anonaine, cypermethrin, and their combination on larvae and engorged

324   females of *Rhipicephalus microplus*.

Treatment	Larval immersion test			Adult immersion test		
	LC_{50} (mg/mL)	CI 95%	R^2	% Rovip	%Rhatch	C%
Anonaine (0.1 mg/mL)*	-	-	-	3.73±9.90[a]	-	6.24±8.74[a]
Anonaine (0.5 mg/mL)*	-	-	-	17.69±24.10[a]	37.4±7.1[a]	14.26±25.82[a]
Cypermethrin (CYP)	0.044[a]	0.038 - 0.050	0.96	62.25±6.76[b]	96.85±0.60[b]	98.85±0.30[b]
CYP + anonaine (0.1 mg/mL)	0.057[b]	0.054 – 0.061	0.99	52.42±15.39[b]	98.65±6.97[b]	99.44±0.28[b]
CYP + anonaine (0.5 mg/mL)	0.022[c]	0.016 - 0.029	0.93	61.25±2.68[b]	94.27±6.97[b]	97.79±2.60[b]

325   * Anonaine had no effect on larvae; LC_{50}: Lethal concentration (mg/mL) for 50% of individuals;
326   CI: 95% confidence interval; R^2: Regression Correlation Coefficient. % Rovip: Percentage of
327   reduction in oviposition; % Rhatch: Percentage of hatching reduction; C%: Control percentage.
328   Mean± standard deviation. The same superscript letter in the same column indicates that the mean
329   does not differ significantly at p <0.05.
330

331   **4. Discussion**

332   The search for alternatives to control *R. microplus* is one of the biggest challenges

333   for cattle production as illustrated by several reports about emergence of multi-resistant

334   tick populations (Tavares et al., 2022). This study presents *in silico* and *in vitro* evidence

335   of inhibition of *R. microplus* GST by the purified plant alkaloid anonaine, which

336   improved the cypermethrin *in vitro* larvicidal effect.

337   First, the potential of anonaine to inhibit *R. microplus* GST was evaluated *in silico*

338   after the construction and validation of an *R. microplus* GST structure model

(Supplementary Figure 2). The Ramachandran plot of the tick GST modelled structure

showed 91% of the residues in the most favorable regions (Supplementary Figure 2). This

result was adequate since a percentage of CORE residues higher than 90% indicates that

a model has a good resolution (Laskowski et al., 2013).

To identify the best docking protocol, a re-docking experiment was carried out with

the human GST and the N11 inhibitor, and an RMSD of 1.9 Å was obtained. The

algorithms are valid if the re-docking results have an RSMD less than 2 Å from the

original structure (Hecht and Fogel, 2009). After the tick and human GST structures

superimposition, the RMSD obtained was 1.1 Å. The percentage of amino-acid identity

between the two protein sequences is a mere 28.8%, but the low RMSD value indicates

high structural similarity between the two structures. Additionally, protocols for

molecular docking consider that 3D structures of two protein sequences having an identity

higher than 25% are sufficiently similar for comparative docking studies (Shen et al.,

2013). Based on these results, the same docking protocol was used for both GST

structures in this study. According to the molecular docking results, anonaine would have

a higher affinity for *R. microplus* GST than for human GST (Figure 1 and Supplementary

Figure 1).

The residues of the human GST interacting with anonaine were not the same as the

R. microplus GST interacting residues (Supplementary Figure 1 and Supplementary

Table 1), suggesting a different mode of ligation between anonaine with the parasite and

with the mammalian enzymes. This could thus be helpful for the development of selective

drugs (Ahmad et al., 2008, Moraes et al., 2011).

The predicted ADMET properties of anonaine with different parameters analyzed by

the PreADMET tool shown in Supplementary Table 2, suggest that anonaine has

moderate toxicity and no carcinogenic potential. All values obtained in the results with

364 anonaine were compared to standard values reported in the literature (Ames et al., 1972;

365 Yee, 1997; Van De Waterbeemd and Gifford, 2003; Alliance, 2016; Wadapurkar et al.,

366 2018; Ferreira et al., 2020; Pereira, 2021; Tong et al., 2021). Also, it is suggested that

367 natural alkaloid anonaine is less toxic to mammals than cypermethrin. However,

368 additional studies to elucidate anonaine's mechanism of action, pharmacology, toxicity,

369 and pharmacokinetics are necessary to explore possibilities for its optimization and

370 clinical application of derived products.

371 Alkaloids exhibit multiple biological activities, and there are already several drugs

372 commercially available derived from natural plant alkaloids (Debnath et al., 2018). In

373 this study, anonaine was isolated from leaves of *Annona crassiflora* in an amount and

374 quality adequate to perform the immersion tests (Figure 2).

375 The inhibition of r*Rm*GST activity increased with the increase in the anonaine

376 concentration (Figure 4), revealing the capacity of an alkaloid to inhibit tick GST. A

377 similar result has been reported for alkaloids isolated from the plant *Rauvolfia tetraphylla*

378 (Linnaeus, 1753) that inhibited the GST activity of *Setaria cervi* up to 64% at 1 mg/mL

379 (Behera and Bhatnagar, 2019).

380 The most important finding was that the combination of anonaine (0.5 mg/mL)

381 with cypermethrin increased the toxicity of the pyrethroid 2-fold against *R. microplus*

382 larvae (Table 1). Plant alkaloids have been demonstrated to possess acaricidal activity

383 against *R. microplus* and *R. annulatus* (Divya et al., 2014; Silva et al., 2021). For instance,

384 alkaloids and glycosides detected in a *Datura metel* extract had synergistically inhibitory

385 effects against *R. microplus* engorged females (Ghosh et al., 2015). Moreover, an

386 alkaloid-rich fraction from *Prosopis juliflora* (Sargent 1902) was responsible for activity

387 against adult females of *R. microplus* (Lima et al., 2020). In addition, this alkaloid-rich

388 fraction was more active on larvae than on adults. However, many approaches, including

chemical and formulation modifications can be utilized to improve drug properties and increase the biological effect against adult ticks. The different susceptibility between *R. microplus* larvae and adults for the alkaloids may be explained since larvae have a thinner cuticle than adults (Conceicao et al., 2017; Cruz et al., 2016). In this study, anonaine alone was ineffective against *R. microplus* larvae. Our result suggests that this alkaloid, by inhibiting the *R. microplus* GST, interferes negatively with the cypermethrin detoxification system of the tick, improving the larvicidal effect of the pyrethroid.

Although the larvae phase is widely used to evaluate the acaricidal activity of compounds derived from plants *in vitro*, the efficacy of the compounds can vary according to the developmental phase of the tick (Rosado-Aguilar et al., 2017). For instance, the wax layer is thicker in adults than in larvae, increasing the sequestration of compounds within the wax and reducing their efficacy (Adenubi et al., 2018). This study demonstrated the increase of anti-larval activity of cypermethrin by anonaine. Despite the protective effects against larva, the cypermethrin-anonaine combination needs improvement to increase activity against all life stages of the tick.

5. Conclusion

This study shows, *in silico* and *in vitro*, the capacity of anonaine to inhibit the r*Rm*GST activity. The immersion tests revealed that anonaine can increase the toxic activity of cypermethrin against *R. microplus* larvae.

References

Adenubi, O.T., Ahmed, A.S., Fasina, F.O., McGaw, L.J., Eloff, J.N., Naidoo, V., 2018. Pesticidal plants as a possible alternative to synthetic acaricides in tick control: A systematic review and meta-analysis. Industrial Crops Products 123, 779-806.

Ahmad, R., Srivastava, A.K., Walter, R.D., 2008. Purification and biochemical characterization of cytosolic glutathione-S-transferase from filarial worms *Setaria cervi*. Comparative Biochemistry Physiology Part B: Biochemistry Molecular Biology 151, 237-245.

Alliance, D., 2016. Estudo químico, predições *in silico* das propriedades ADME/TOX e atividade larvicida do óleo essencial da raiz *Philodendron deflexum* Poepp. Ex Schott sobre *Aedes egypti* Linneu e *Anopheles albirtasis* sl, Department of Graduation Graduation Program in Health Sciences - Ppgcs. Federal University Of Amapa., Macapá - Ap. Brazil., pp. 1-53.

Alvarez, J.C., 2004. High-throughput docking as a source of novel drug leads. Current Opinion in Chemical Biology 8, 365-370.

Ames, B.N., Gurney, E., Miller, J.A., Bartsch, H., 1972. Carcinogens as frameshift mutagens: metabolites and derivatives of 2-acetylaminofluorene and other aromatic amine carcinogens. Proceedings of the National Academy of Sciences of the U.S.A. 69, 3128-3132.

436 Azeez, S., Babu, R.O., Aykkal, R., Narayanan, R., 2012. Virtual screening and *in vitro*
437 assay of potential drug like inhibitors from spices against glutathione-S-transferase of
438 filarial nematodes. Journal of Molecular Modelling 18, 151-163.

439 Behera, D.R., Bhatnagar, S., 2019. *In-vitro* and *in silico* efficacy of isolated alkaloid
440 compounds from *Rauvolfia tetraphylla* L. against bovine filarial parasite *Setaria cervi*: a
441 drug discovery approach. Journal of Parasitic Diseases 43, 103-112.

442 Bennett, G., 1974. Oviposition of *Boophilus microplus* (Canestrini) (Acarida: Ixodidae).
443 I. Influence of tick size on egg production. Acarologia 16, 52-61.

444 Braz, V., Gomes, H., Galina, A., Saramago, L., Braz, G., da Silva Vaz Jr, I., Logullo, C.,
445 da Fonseca, R.N., Campos, E., Moraes, J., 2019. Inhibition of energy metabolism by 3-
446 bromopyruvate in the hard tick *Rhipicephalus microplus*. Comparative Biochemistry
447 Physiology Part C: Toxicology Pharmacology. 218, 55-61.

448 Chen, C.-Y., Chang, F.-R., Pan, W.-B., Wu, Y.-C., 2001. Four alkaloids from *Annona*
449 *cherimola*. Phytochemistry 56, 753-757.

450 Choubey, S.K., Jeyaraman, J., 2016. A mechanistic approach to explore novel HDAC1
451 inhibitor using pharmacophore modelling, 3D-QSAR analysis, molecular docking,
452 density functional and molecular dynamics simulation study. Journal of Molecular
453 Graphics Modelling 70, 54-69.

454 Conceicao, R.S., Carneiro, M.M.A.d.A., Reis, I.M.A., Branco, A., Vieira, I.J.C., Braz-
455 Filho, R., Botura, M.B., 2017. *In vitro* acaricide activity of *Ocotea aciphylla* (Nees)
456 Mez.(Lauraceae) extracts and identification of the compounds from the active fractions.
457 Ticks and Tick-borne Diseases 8, 275-282.

458 Cruz, P.B., Barbosa, A.F., Zeringóta, V., Melo, D., Novato, T., Fidelis, Q.C., Fabri, R.L.,
459 de Carvalho, M.G., Sabaa-Srur, A.U.O., Daemon, E., 2016. Acaricidal activity of
460 methanol extract of *Acmella oleracea* L.(Asteraceae) and spilanthol on *Rhipicephalus*
461 *microplus* (Acari: Ixodidae) and *Dermacentor nitens* (Acari: Ixodidae). Veterinary
462 Parasitology 228, 137-143.

463 Cuevas-Hernández, R.I., Girard, R.M., Martínez-Cerón, S., Santos da Silva, M., Elias,
464 M.C., Crispim, M., Trujillo-Ferrara, J.G., Silber, A.M., 2020. A fluorinated
465 phenylbenzothiazole arrests the *Trypanosoma cruzi* cell cycle and diminishes the
466 infection of mammalian host cells. Antimicrobial Agents Chemotherapy 64, 1-16.

467 Debnath, B., Singh, W.S., Das, M., Goswami, S., Singh, M.K., Maiti, D., Manna, K.,
468 2018. Role of plant alkaloids on human health: A review of biological activities. Materials
469 Today Chemistry 9, 56-72.

470 Divya, T., Soorya, V., Amithamol, K., Juliet, S., Ravindran, R., Nair, S., Ajithkumar, K.,
471 2014. Acaricidal activity of alkaloid fractions of *Leucas indica* Spreng against
472 *Rhipicephalus (Boophilus) annulatus* tick. Tropical Biomedicine 31, 46-53.

473 Drummond, R., et al., Ernst, S., Trevino, J., Gladney, W., Graham, O., 1973. *Boophilus*
474 *annulatus* and *B. microplus*: laboratory tests of insecticides. Journal of Economic
475 Entomology 66, 130-133.

476 Ferreira, G.G., do Nascimento Brandão, D.L., Dolabela, M.F., 2020. Predição do
477 comportamento farmacocinético, toxicidade e de atividades biológicas de alcaloides
478 isolados de *Geissospermum laeve* (Vell.) Miers. Research, Society Development 9, 1-23.

479   Ganesan, A., 2016. Multitarget drugs: an epigenetic epiphany. ChemMedChem 11, 1227-
480   1241.

481   Ghosh, S., Gupta, S., Kumar, K.A., Sharma, A.K., Kumar, S., Nagar, G., Kumar, R., Paul,
482   S., Fular, A., Chigure, G., 2017. Characterization and establishment of a reference
483   deltamethrin and cypermethrin resistant tick line (IVRI-IV) of *Rhipicephalus (Boophilus)*
484   *microplus*. Pesticide Biochemistry and Physiology 138, 66-70.

485   Ghosh, S., Tiwari, S.S., Kumar, B., Srivastava, S., Sharma, A.K., Kumar, S.,
486   Bandyopadhyay, A., Julliet, S., Kumar, R., Rawat, A., 2015. Identification of potential
487   plant extracts for anti-tick activity against acaricide resistant cattle ticks, *Rhipicephalus*
488   *(Boophilus) microplus* (Acari: Ixodidae). Experimental Applied Acarology 66, 159-171.

489   Grisi, L., Leite, R.C., Martins, J.R.d.S., Barros, A.T.M.d., Andreotti, R., Cançado, P.H.D.,
490   León, A.A.P.d., Pereira, J.B., Villela, H.S., 2014. Reassessment of the potential economic
491   impact of cattle parasites in Brazil. Revista Brasileira de Parasitologia Veterinária 23,
492   150-156.

493   Guneidy, R.A., Shahein, Y.E., Abouelella, A.M., Zaki, E.R., Hamed, R., 2014. Inhibition
494   of the recombinant cattle tick *Rhipicephalus (Boophilus) annulatus* glutathione S-
495   transferase. Ticks and Tick-borne Diseases 5, 528-536.

496   Habig, W.H., Pabst, M.J., Fleischner, G., Gatmaitan, Z., Arias, I.M., Jakoby, W.B., 1974.
497   The identity of glutathione S-transferase B with ligandin, a major binding protein of liver.
498   Proceedings of the National Academy of Sciences of the U.S.A. 71, 3879-3882.

499 Hall Jr, D.C., Ji, H.-F., 2020. A search for medications to treat COVID-19 via *in silico*

500 molecular docking models of the SARS-CoV-2 spike glycoprotein and 3CL protease.

501 Travel Medicine and Infectious Disease 35, 1-13.

502 Hamza, I., Dailey, H.A., 2012. One ring to rule them all: trafficking of heme and heme

503 synthesis intermediates in the metazoans. Biochimica et Biophysica Acta -Molecular Cell

504 Research 1823, 1617-1632.

505 Hanwell, M.D., Curtis, D.E., Lonie, D.C., Vandermeersch, T., Zurek, E., Hutchison,

506 G.R., 2012. Avogadro: an advanced semantic chemical editor, visualization, and analysis

507 platform. Journal of Cheminformatics 4, 1-17.

508 Hecht, D., Fogel, G.B., 2009. A novel *in silico* approach to drug discovery via

509 computational intelligence. Journal of Chemical Information Modelling 49, 1105-1121.

510 Kaewmongkol, S., Kaewmongkol, G., Inthong, N., Lakkitjaroen, N., Sirinarumitr, T.,

511 Berry, C., Jonsson, N., Stich, R., Jittapalapong, S., 2015. Variation among Bm86

512 sequences in *Rhipicephalus (Boophilus) microplus* ticks collected from cattle across

513 Thailand. Experimental and Applied Acarology 66, 247-256.

514 Kelley, L.A., Mezulis, S., Yates, C.M., Wass, M.N., Sternberg, M.J., 2015. The Phyre2

515 web portal for protein modelling, prediction and analysis. Nature Protocols 10, 845-858.

516 Klafke, G.M., Sabatini, G.A., Thais, A., Martins, J.R., Kemp, D.H., Miller, R.J.,

517 Schumaker, T.T., 2006. Larval immersion tests with ivermectin in populations of the

518 cattle tick *Rhipicephalus (Boophilus) microplus* (Acari: Ixodidae) from State of Sao

519 Paulo, Brazil. Veterinary Parasitology 142, 386-390.

520   Kumar, R., Nagar, G., Sharma, A.K., Kumar, S., Ray, D., Chaudhuri, P., Ghosh, S., 2013.

521   Survey of pyrethroids resistance in Indian isolates of *Rhipicephalus (Boophilus)*

522   *microplus:* identification of C190A mutation in the domain II of the para-sodium channel

523   gene. Acta Tropica 125, 237-245.

524   Kwang, L.S., 2005. *In silico* high-throughput screening for ADME/Tox properties:

525   PreADMET program, Abstr Conf Comb Chem Jpn 21, 22-28.

526   Laskowski, R.A., Furnham, N., Thornton, J.M., 2013. The Ramachandran plot and

527   protein structure validation, Biomolecular Forms and Functions: A Celebration of 50

528   Years of the Ramachandran Map. World Scientific 1, 62-75.

529   Laskowski, R.A., MacArthur, M.W., Moss, D.S., Thornton, J.M., 1993. PROCHECK: a

530   program to check the stereochemical quality of protein structures. Journal of Applied

531   Crystallography 26, 283-291.

532   Li, H.-T., Wu, H.-M., Chen, H.-L., Liu, C.-M., Chen, C.-Y., 2013. The pharmacological

533   activities of (−)-anonaine. Molecules 18, 8257-8263.

534   Lima, H.G.d., Santos, F.O., Santos, A.C.V., Silva, G.D.d., Santos, R.J.d., Carneiro,

535   K.d.O., Reis, I.M.A., Estrela, I.d.O., Freitas, H.F.d., Bahiense, T.C., 2020. Anti-tick effect

536   and cholinesterase inhibition caused by *Prosopis juliflora* alkaloids: *in vitro* and *in silico*

537   studies. Revista Brasileira de Parasitologia Veterinária 29, 1-15.

538   Lopes, W.D.Z., Teixeira, W.F.P., de Matos, L.V.S., Felippelli, G., Cruz, B.C., Maciel,

539   W.G., Buzzulini, C., Fávero, F.C., Soares, V.E., de Oliveira, G.P., 2013. Effects of

540   macrocyclic lactones on the reproductive parameters of engorged *Rhipicephalus*

541 *(Boophilus) microplus* females detached from experimentally infested cattle.
542 Experimental Parasitology 135, 72-78.

543 Mangoyi, R., Hayeshi, R., Ngadjui, B., Ngandeu, F., Bezabih, M., Abegaz, B.,
544 Razafimahefa, S., Rasoanaivo, P., Mukanganyama, S., 2010. Glutathione transferase
545 from *Plasmodium falciparum*–Interaction with malagashanine and selected plant natural
546 products. Journal of Enzyme Inhibition and Medicinal Chemistry 25, 854-862.

547 Mannervik, B., 1985. The isoenzymes of glutathione transferase. Advances in
548 Enzymology and Related Areas of Molecular Biology 57, 357-417.

549 Mannervik, B., Helena Danielson, U., Ketterer, B., 1988. Glutathione transferases—
550 structure and catalytic activit. Critical Reviews in Biochemistry 23, 283-337.

551 Moraes, J., Arreola, R., Cabrera, N., Saramago, L., Freitas, D., Masuda, A., da Silva Vaz
552 Jr, I., de Gomez-Puyou, M.T., Perez-Montfort, R., Gomez-Puyou, A., 2011. Structural
553 and biochemical characterization of a recombinant triosephosphate isomerase from
554 *Rhipicephalus (Boophilus) microplus*. Insect Biochemistry and Molecular Biology 41,
555 400-409.

556 Ndawula Jr, C., Sabadin, G.A., Parizi, L.F., Vaz Jr, I. S, 2019. Constituting a glutathione
557 S-transferase-cocktail vaccine against tick infestation. Vaccine 37, 1918-1927.

558 Olivares-Illana, V., Pérez-Montfort, R., López-Calahorra, F., Costas, M., Rodríguez-
559 Romero, A., Tuena de Gómez-Puyou, M., Gómez Puyou, A., 2006. Structural differences
560 in triosephosphate isomerase from different species and discovery of a
561 multitrypanosomatid inhibitor. Biochemistry 45, 2556-2560.

562 Ozelame, K.P.C., Mattia, M.M.C., Silva L.A.D., Randall, L.M., Corvo I., Saporiti, T.,

563 Seixas, A., da Silva Vaz, I Jr, Alvarez, G., 2022. Novel tick glutathione transferase

564 inhibitors as promising acaricidal compounds. Ticks and Tick-borne Diseases 13, 1-7.

565 Pereira, G., Bruno., 2021. *In silico* pharmacology studies of phenolic esters designed to

566 obtain tyrosine kinase inhibitors, Chemistry department. Federal Technological

567 University of Paraná, Campo Mourão- PR., pp. 1-67.

568 Prade, L., Huber, R., Manoharan, T.H., Fahl, W.E., Reuter, W., 1997. Structures of class

569 pi glutathione S-transferase from human placenta in complex with substrate, transition-

570 state analogue and inhibitor. Structure 5, 1287-1295.

571 Roche, J., Bertrand, P., 2016. Inside HDACs with more selective HDAC inhibitors.

572 European Journal of Medicinal Chemistry 121, 451-483.

573 Roditakis, E., Roditakis, N.E., Tsagkarakou, A., 2005. Insecticide resistance in *Bemisia*

574 *tabaci* (Homoptera: Aleyrodidae) populations from Crete. Pest Management Science 61,

575 577-582.

576 Rosado-Aguilar, J., Arjona-Cambranes, K., Torres-Acosta, J., Rodríguez-Vivas, R.,

577 Bolio-González, M., Ortega-Pacheco, A., Alzina-López, A., Gutiérrez-Ruiz, E.,

578 Gutiérrez-Blanco, E., Aguilar-Caballero, A., 2017. Plant products and secondary

579 metabolites with acaricide activity against ticks. Veterinary Parasitology 238, 66-76.

580 Saramago, L., Gomes, H., Aguilera, E., Cerecetto, H., González, M., Cabrera, M.,

581 Alzugaray, M.F., Vaz Junior, I. S., Nunes da Fonseca, R., Aguirre-López, B., 2018. Novel

582 and selective *Rhipicephalus microplus* triosephosphate isomerase inhibitors with

583 acaricidal activity. Veterinary Sciences 5, 1-19.

584 Shen, W. J. Zhang, H. Fang, R. Perkins, W. Tong, H. Hong., 2013. Homology modelling,

585 molecular docking, and molecular dynamics simulations elucidated α-fetoprotein binding

586 modes, BMC Bioinformatics 14, 1–14.

587 Sievers, F., Wilm, A., Dineen, D., Gibson, T.J., Karplus, K., Li, W., Lopez, R.,

588 McWilliam, H., Remmert, M., Söding, J., 2011. Fast, scalable generation of high-quality

589 protein multiple sequence alignments using Clustal Omega. Molecular Systems Biology

590 7, 1-6.

591 Silva, G.D., de Lima, H.G., de Freitas, H.F., da Rocha Pita, S.S., dos Santos Luz, Y., de

592 Figueiredo, M.P., Uzeda, R.S., Branco, A., Costa, S.L., Batatinha, M.J.M., 2021. *In vitro*

593 and *in silico* studies of the larvicidal and anticholinesterase activities of berberine and

594 piperine alkaloids on *Rhipicephalus microplus*. Ticks and Tick-borne Diseases 12, 1-6.

595 Tavares, C.P., Sousa, I.C., Gomes, M.N., Miró, V., Virkel, G., Lifschitz, A., Costa-Junior,

596 L.M., 2022. Combination of cypermethrin and thymol for control of *Rhipicephalus*

597 *microplus:* Efficacy evaluation and description of an action mechanism. Ticks and Tick-

598 borne Diseases 13, 1-8.

599 Tong, J.-B., Luo, D., Bian, S., Zhang, X., 2021. Structural investigation of

600 tetrahydropteridin analogues as selective PLK1 inhibitors for treating cancer through

601 combined QSAR techniques, molecular docking, and molecular dynamics simulations.

602 Journal of Molecular Liquids 335, 1-17.

603 Van De Waterbeemd, H., Gifford, E., 2003. ADMET *in silico* modelling: towards

604 prediction paradise? Nature Reviews Drug Discovery 2, 192-204.

605   Vaz Jr, I.S., Lermen, T.T., Michelon, A., Ferreira, C.A.S., de Freitas, D.R.J., Termignoni,

606   C., Masuda, A., 2004. Effect of acaricides on the activity of a *Boophilus microplus*

607   glutathione S-transferase. Veterinary Parasitology 119, 237-245.

608   Wadapurkar, R.M., Shilpa, M., Katti, A.K.S., Sulochana, M., 2018. *In silico* drug design

609   for *Staphylococcus aureus* and development of host-pathogen interaction network.

610   Informatics in Medicine Unlocked 10, 58-70.

611   Wadood, A., Ahmed, N., Shah, L., Ahmad, A., Hassan, H., Shams, S., 2013. *In-silico*

612   drug design: An approach which revolutionarised the drug discovery process. OA Drug

613   Design and Delivery 1, 1-4.

614   Xavier, M., Sehnem Heck, G., Boff de Avila, M., Maria Bernhardt Levin, N., Oliveira

615   Pintro, V., Lemes Carvalho, N., Filgueira de Azevedo, W., 2016. SAnDReS a

616   computational tool for statistical analysis of docking results and development of scoring

617   functions. Combinatorial Chemistry and High Throughput Screening 19, 801-812.

618   Yee, S., 1997. *In vitro* permeability across Caco-2 cells (colonic) can predict in vivo

619   (small intestinal) absorption in man—fact or myth. Pharmaceutical Research 14, 763-

620   766.

621   Yusuf, D., Davis, A.M., Kleywegt, G.J., Schmitt, S., 2008. An alternative method for the

622   evaluation of docking performance: RSR vs RMSD. Journal of Chemical Information and

623   Modelling 48, 1411-1422.
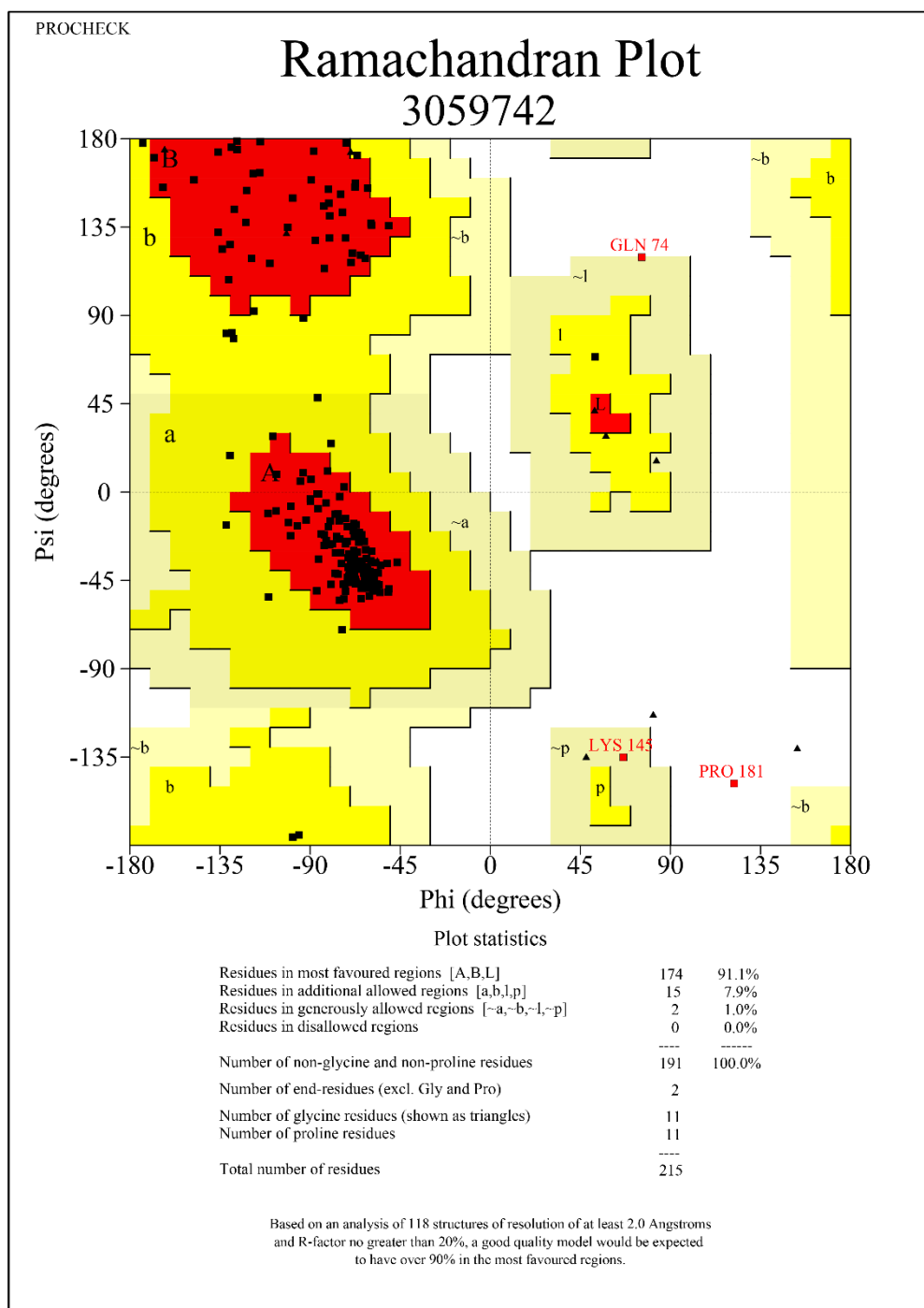
624

625   **Supplementary data**

626
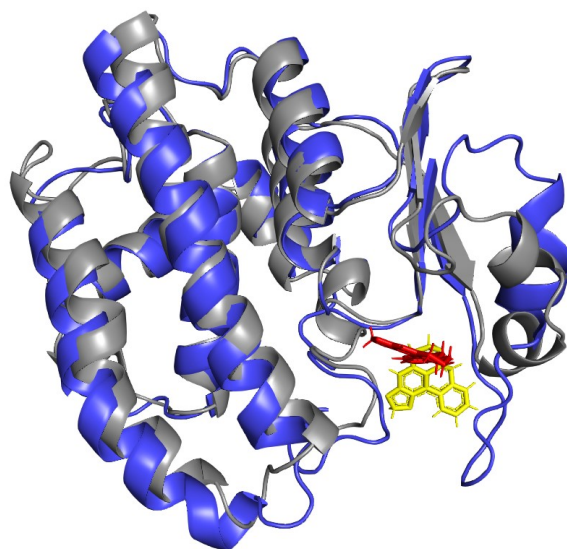
627

628   **Supplementary Figure 1** A) Cartoon representation of the structures of glutathione S-transferase

629   (GST) of *Rhipicephalus microplus* (in blue) and human (PDB:3IE3 - in grey) with anonaine (best

630   pose after molecular docking) coloured in yellow and red, respectively.

631

632

Supplementary Figure 2. Ramachandran plot of the predicted glutathione S-transferase (GST) structure of *Rhipicephalus microplus* (the red, dark yellow, and light-yellow regions represent the most favored, allowed, and generously allowed regions).

639   **Supplementary Table 1**. Comparison of the amino acids of the *R. microplus* GST and

640   the human GST interacting with anonaine, as determined by molecular docking.

Ligand	Amino acids	
	GST - *R. microplus*	**GST - Human**
Anonaine	Thr 10, Thr 11, Ala 12, Tyr 35, Glu 36, Phe 37, Gly 38, Pro 39, Ala 40, Tyr 43, Pro 209, Met 211, Ala 212, Pro 213	Tyr 7, Phe 8, Pro 9, Val 10, Val 33, Thr 34, Val 35, Trp 38, Tyr 108, Pro 202, Gly 205

641   Thr = Threonine; Ala = Alanine; Tyr = Tyrosine; Glu = Glutamic acid; Phe = Phenylalanine; Gly

642   = Glycine; Pro = Proline; Met = Methionine; Val = Valine; Trp = Tryptophan are anonaine-

643   interacting residues taken from the human and *R. microplus* GST structures.

644

645

646

647

648

649

650

651

652

653

654

655

656

657

658

659

660 **Supplementary Table 2.** Predicted ADMET properties of the anonaine.

ID	Anonaine
Absorption	
Caco2	47.681
HIA	96.493
MDCK	177.096
Pgp_inh	Non
PPB	65.565
PWS (mg/L)	57.025
Skin_Permeability	-4.113
Distribution	
BBB	0.9849
Metabolism	
CYP2C19_inh	Non
CYP2C9_inh	Non
CYP2D6_inh	Inhibitor
CYP2D6_sub	Substrate
CYP3A4_inh	Non
CYP3A4_sub	Weak substr.
Toxicity	
algae_at	0.055948
Ames_test	Mutagen
Carcino_Mo	Negative
Carcino_Rat	Negative
daphnia_at	0.147588

hERG_inh	Medium_risk
medaka_at	0.0328064
minnow_at	0.0519424

661 **BBB -** Blood-Brain Barrier (C.brain/C.blood); **Caco-2 -** Caco2-cell model; **HIA** - Human

662 Intestinal Absorption model (HIA, %); **MDCK -** Madin-Darby Canine Kidney (nm/sec);

663 **PGP_inh -** P-glycoprotein inhibitor; **PPB –** Plasma Protein Binding (%); **PWS** – Pure water

664 solubility (mg/L); **Skin Permeability-** Skin permeability in cm/hour. **Algae at -** algae test (mg/L);

665 **Ames Test -** Ames Salmonella; **CYP -** Cytochrome P450; **Carcino M -** carcinogenesis test in the

666 mouse; **Carcino R -** carcinogenesis test in rats; **Daphnia at -** test on crustacean daphnia; **hERG**

667 **Inhib.** - hERG-controlled potassium channel inhibition; **Medaka_at -** test on medaka fish;

668 **Minnow_at -** test on small freshwater fish.

669

670

671

672

673

674

675

676

677

678

679

680

681

682

683

684

685

686

687

688

689

690

691

692